# Supersonic molecular jet studies of the pyrazine and pyrimidine dimers

J. Wanna, J. A. Menapace, and E. R. Bernstein

Citation: The Journal of Chemical Physics **85**, 777 (1986); doi: 10.1063/1.451285
View online: http://dx.doi.org/10.1063/1.451285
View Table of Contents: http://aip.scitation.org/toc/jcp/85/2
Published by the American Institute of Physics

# Supersonic molecular jet studies of the pyrazine and pyrimidine dimers[a)]

J. Wanna, J. A. Menapace, and E. R. Bernstein
*Department of Chemistry, Condensed Matter Sciences Laboratory, Colorado State University, Fort Collins, Colorado 80523*

(Received 13 December 1985; accepted 8 April 1986)

Mass selected optical spectra for the first excited singlet $n\pi^*$ states of the pyrazine and pyrimidine dimers are presented. The species are created in a pulsed supersonic jet expansion. The spectra are analyzed based on ionization energy, vibronic structure, and relative energy with respect to the isolated monomer (cluster spectroscopic shift). Calculations of binding energy and geometry for these dimers are carried out employing a Lennard-Jones (6-12-1) and hydrogen bonding (10-12-1) potential. In the case of pyrazine, calculations and experiments agree that both parallel planar hydrogen bonded and perpendicular dimers are present in the expansion. The calculations also predict a parallel stacked and 90° rotated pyrazine dimer which is not observed. This latter species most likely forms an excimer in the excited state with a short lifetime and a highly red shifted broad spectrum. In the case of pyrimidine, calculations yield four planar hydrogen bonded species and a parallel stacked and displaced species. The spectra for the pyrimidine dimer are consistent with these configurations, in agreement with the calculations. No perpendicular configuration is calculated for the pyrimidine dimer and no spectroscopic features require postulating the existence of such a configuration. To explore further the agreement between calculated and experimental results for aromatic dimers, calculations are also presented for the tetrazine dimer. Three calculated geometries are obtained for the tetrazine dimer: a parallel stacked and 90° rotated species, a planar hydrogen bonded species, and a perpendicular species. Experimental spectra and calculations are in basic agreement for all dimers studied and, in general, support one another.

## I. INTRODUCTION

Molecular dimers are of interest for a number of reasons. They can serve as model systems for condensed phase structure, dynamics, and nucleation and growth. Vibrational dynamics and reactions can be studied in clusters through the observation of vibrational dephasing or intramolecular vibrational redistribution (IVR) and vibrational predissociation (VP). Dimers also provide a model for higher order (i.e., secondary, tertiary, etc.) structure of more complex, flexible molecules. Finally, these small clusters can be treated as a new, weakly coupled state of matter appropriate in its own right for investigation and focused attention.

Small clusters or dimers are best studied by molecular jet techniques,[1-6] as the species are thereby isolated and free of extraneous perturbations. Of the molecular supersonic jet spectroscopy techniques available, the most useful is two-color time of flight mass spectroscopy[1] (2-color TOFMS) because many different clusters [e.g., dimers, trimers, dimers $(He)_n$, etc.] are simultaneously produced in the expansion process. Two-color TOFMS selects a cluster of particular mass, does not allow fragmentation of clusters to take place, thus maintaining mass integrity of the clusters, and yields a plot of cluster ion intensity in the chosen mass channel as a function of the cluster absorption spectrum.

Dimers of benzene, toluene, and benzene–toluene have been studied in our laboratory using the 2-color TOFMS technique.[1] Coupled with the experimental findings, a potential energy calculation of the structure and binding energy of these dimers based on an exponential-six (exp-6) function has also been reported.[2] Spectroscopic data and potential energy calculations have been analyzed to arrive at a set of consistent geometries for these dimers. The benzene dimer is suggested to have a parallel displaced structure and the toluene and toluene–benzene dimers are suggested to have both parallel displaced and perpendicular geometries. The benzene dimer characterization rests on isotopic substitution, absence of resolved splittings at the cluster $0_0^0$, observation of only one feature, respectively, for $(C_6H_6)_2$, $(C_6D_6)_2$, and $C_6H_6C_6D_6$ at the cluster $0_0^0$, and calculations employing the observed molecular quadrupole moment of $C_6H_6$ to set partial and atomic charges and multipolar terms. In all instances, the experiments and calculations appear to arrive at self-consistent and independent conclusions which are in agreement with one another.

Molecular jet studies of other isolated dimers have also been reported. Rotationally resolved fluorescence excitation and dispersed emission spectra of tetrazine,[3] phenyltetrazine,[4] and dimethyltetrazine[5] dimers have been reported. Hydrogen bonded benzoic acid[6] and benzoic acid–*p*-toluic acid[7] dimers have also been studied.

In this paper we report rotationally resolved 2-color TOFMS of pyrazine and pyrimidine isolated molecules at a resolution of 0.08 $cm^{-1}$. Unfortunately, this is insufficient resolution to obtain rotationally resolved 2-color TOFMS of the pyrazine and pyrimidine dimers. Computer simulations, based on a reasonable symmetric top algorithm, predict a resolution of at least 0.005 $cm^{-1}$ (150 MHz) is needed to observe rotational structure for the dimers, assuming they are rigid.

[a)] Supported in part by grants from ONR and the Philip Morris Corporation.

 0021-9606/86/140777-08$02.10 © 1986 American Institute of Physics 

In addition to the experimental spectroscopic methods used to study these dimers, potential energy calculations utilizing a Lennard-Jones (LJ; 6-12-1) potential are performed to yield minimum energy geometries and binding energies. This potential form is replaced with a LJ-hydrogen bonding (HB; 10-12-1) form for the appropriate set of atoms. The calculation and parameters employed are discussed and presented in an earlier publication.[8] These potentials, with literature parameter values, give the same results as the exp-6 with dipole–dipole, dipole–quadrupole, and quadrupole–quadrupole terms for the benzene, toluene, and benzene-toluene (and pyrazine and pyrimidine) dimers. The major advantage of the LJ form presently used in our studies is that more atomic parameters are available in the literature[9] and experimental multipole moments are not required for each system.

Dimer geometry is determined through analysis of experimental (e.g., shifts, ionization energies, origin identification, vibronic analyses, etc.) and calculational results.

## II. EXPERIMENTAL PROCEDURES

A pulsed valve supersonic molecular jet system is used to generate the dimers. The pulsed valve is mounted in the mass spectroscopy chamber of a two chambered vaccum system. Since the duty cycle of the valve is roughly $10^{-3}$, the 10 in. diffusion pump on the chamber and the 6 in. diffusion pump on the TOFMS flight tube adequately handle the gas load and maintain the chamber pressure below $2\times10^{-6}$ Torr. The system is described in previous publications.[1,8] The beam passes through a skimmer and then into the ionization region of a TOFMS. Two separately tunable lasers provide the photons for the $S_0\rightarrow S_1$ transition and the $S_1\rightarrow$cluster ion transition.

Rotationally resolved 2-color TOFMS are obtained through pressure tuning of the grating box of the pump ($S_0\rightarrow S_1$) dye laser oscillator cavity. The output of this laser is narrowed by an etalon placed between the dye cell and the grating in the oscillator cavity. The doubled output from this dye laser is 0.08 $cm^{-1}$ in width. The laser can be scanned over roughly 20 $cm^{-1}$ for a $N_2$ pressure variation of 10 to 1500 Torr.

Pyrazine and pyrimidine are obtained from Aldrich Chemical Company and used without purification. The sample is placed in a trap behind the pulsed valve through which He flows at 120 psig.

The LJ potential energy function and calculational procedure have previously been described.[8] The additional constants needed for this work are the (aromatic) N···H hydrogen bonding values: $B = 8.244\times10^3$ kcal Å$^{10}$/mol and $A' = 3.2897\times10^4$ kcal Å$^{12}$/mol. In order to check the LJ potential form, in particular for the pyrimidine dimer, LJ plus multipolar (i.e., dipole–dipole, dipole–quadrupole, and quadrupole–quadrupole) potential calculations are also performed.[2] The pyrimidine dipole and quadrupole moments[10] are taken to be $-2.97\times10^{-18}$ esu cm and $-1.91\times10^{-26}$ esu cm$^2$, respectively.

Calculations are also reported which simulate the rotational structure of pyrazine and pyrimidine monomers and dimers. A symmetric top model is employed for this fit because it is simple, reasonably accurate, and in general is well suited to the purpose of roughly predicting the unresolved dimer structure. Both molecules are nearly symmetric tops ($\kappa\approx0.9$). The form of the equations and methods employed are given by Herzberg.[11] The rotational temperature achieved in our system is ~2 K. The rotational constants used in the dimer rotational spectra calculations are found from the calculated LJ geometries. The molecular geometries can be found in Ref. 12 for pyrazine and Ref. 13 for pyrimidine.

## III. RESULTS

### A. Pyrazine dimer

The spectrum of the pyrazine dimer at the $0_0^0$ transition is presented in Fig. 1 at two ionization energies, both of which are lower than the minimum ionization (second photon) energy of 44 000 $cm^{-1}$ required to observe the 2-color TOFMS of the pyrazine monomer. Lowering the ionization energy from 43 182 to 42 185 $cm^{-1}$ causes three of the dimer related peaks to disappear: these features are found at $-11.0$, 12.0, and 26.2 $cm^{-1}$ on the scale of Fig. 1. From the nature and appearance of these features, the $+12$ and $+26$ $cm^{-1}$ peaks are quite likely vibrations built on the $-11$ $cm^{-1}$ origin of a given configuration cluster. The intense features that remain at the lower ionization energy are found at $-26.3$, $-5.8$, $+34.1$, and 50.7 $cm^{-1}$. From this variation of ionization energy one can determine that at least two configurations of the pyrazine dimer are present in the su-

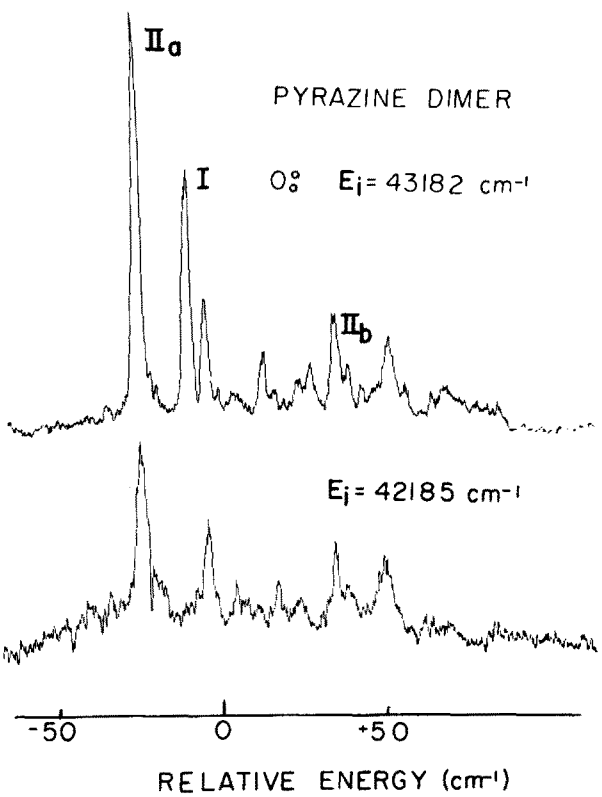


FIG. 1. Two-color TOFMS of the pyrazine dimer in the region of the pyrazine origin at two different ionization energies; top trace at an ionization energy of 43 182 $cm^{-1}$ and the lower trace at an ionization energy of 42 185 $cm^{-1}$. The pyrazine origin at 30 876 $cm^{-1}$ lies at 0 $cm^{-1}$ on the scale of the figure.

personic jet expansion. The pyrazine-$d_4$ dimer $0_0^0$ spectrum at two different ionization energies is presented in Fig. 2: the similarity between the pyrazine-$h_4$ and -$d_4$ dimer spectra is quite striking and reinforces our identification of origins and vdW vibronic features. The features that vanish at lower ionization energy are found at $-11.5$, 11.5, 25.5, and 64.1 $cm^{-1}$ with respect to the pyrazine-$d_4$ $0_0^0$ transition (31 030.4 $cm^{-1}$). These should be compared with the numbers in Table I. The features that remain with lower ionization energy are located at $-26.9$, $-6.5$, 31.0, and 45.9 $cm^{-1}$.

The spectra of the pyrazine dimer at other pyrazine vibronic origins are presented, along with the $0_0^0$ spectrum for comparison, in Fig. 3. The feature at roughly $+61$ $cm^{-1}$ in this figure ($+34.1$ $cm^{-1}$ in Fig. 1) is clearly an additional origin. The energy values and shifts for these features are presented in Table I. Since the pyrazie dimer is still observed at $10a_0^2$, its binding energy is greater than 800 $cm^{-1}$. No other features, appearing in the dimer mass channel, are found within $-400$ $cm^{-1}$ of the pyrazine $0_0^0$ transition. The spectra of the pyrazine-$d_4$ dimer at these other vibronic monomer origins are again very similar to those of the pyrazine-$h_4$ dimer. We concluded from these spectra (not presented) that the third origin for the deuterated dimer lies at 31.0 $cm^{-1}$ from the $0_0^0$ of the deuterated monomer.

Utilizing a Lennard-Jones potential function with a hydrogen bonding form, three configurations for the pyrazine dimer are calculated. Two of these configurations, a planar hydrogen bonded form and a perpendicular form, are displayed in Fig. 4. A parallel, stacked and 90° rotated structure

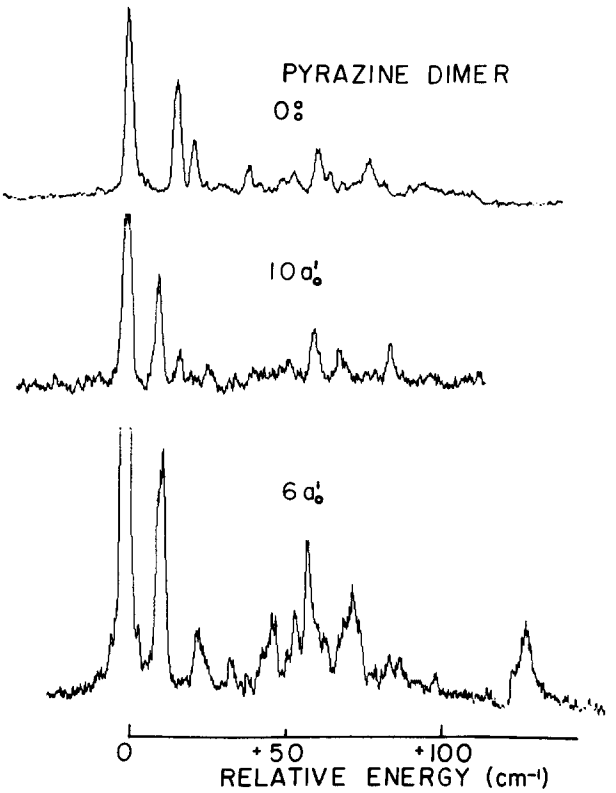


FIG. 3. Two-color TOFMS of the pyrazine dimer in the $0_0^0$, $10a_0^1$, and $6a_0^1$ regions. These spectra are taken at high ($\sim 43\,200$ $cm^{-1}$) ionization energy.

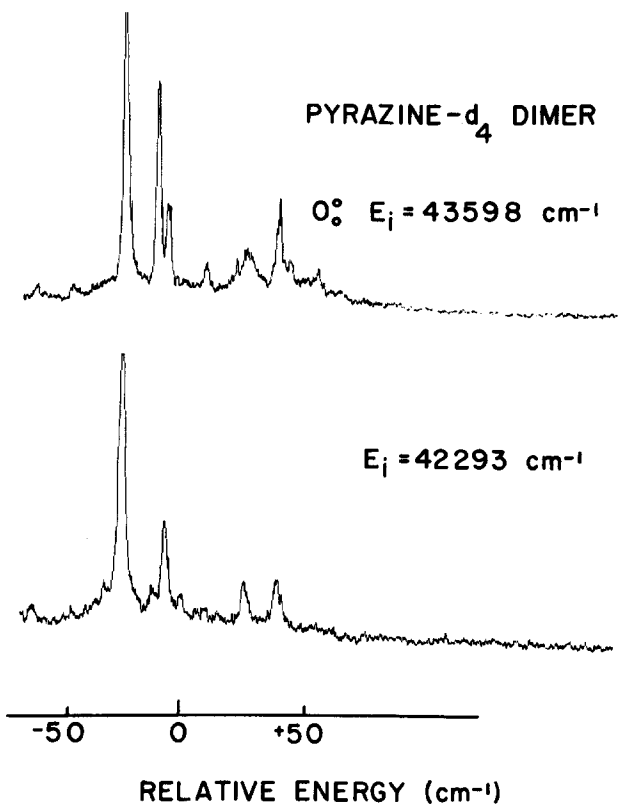


FIG. 2. Two-color TOFMS of the pyrazine-$d_4$ dimer in the region of the pyrazine-$d_4$ origin. Two different ionization energies are presented. The pyrazine-$d_4$ monomer origin lies at 0 $cm^{-1}$ on the scale of the figure. Compare to Fig. 1 for the pyrazine-$h_4$ dimer.

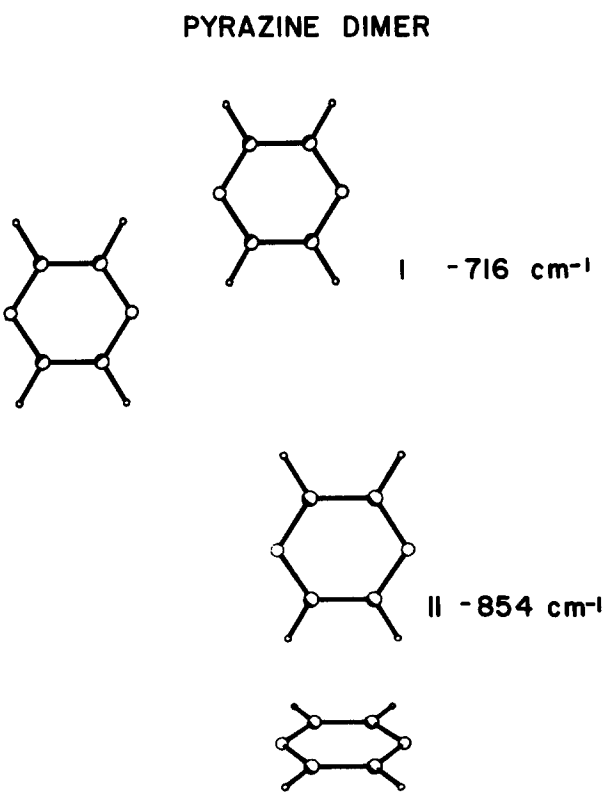


FIG. 4. Minimum energy configurations and binding energies for pyrazine dimer as obtained with a LJ plus HB potential calculation.

is also found. The binding energies for the former two configurations are presented in the figure. In the planar geometry the ring centers are at 5.6 Å from each other and the suggested C–H···N hydrogen bonds are 2.3 Å long. The pyrazine at the stem of the perpendicular configuration is situated in a symmetric position above the base pyrazine, with two of its hydrogens pointing to the base pyrazine nitrogens and equidistant from them. This perpendicular configuration has a 4.6 Å pyrazine center to center separation and apparent 2.6 Å H···N bond lengths.

### B. Pyrimidine dimer

Three segments of the pyrimidine dimer 2-color TOFMS spectrum in the $0_0^0$ region are displayed in Fig. 5 for two different ionization energies. Based only on the position and appearance of these segments we suggest that the features at $-168$ and $+296$ cm$^{-1}$ are each associated with different geometries. The grouping of features in the $+170$ cm$^{-1}$ region must be associated with more than one dimer configuration, as these eight sharp, relatively intense features are clearly not vdW vibronic progressions built on a single $0_0^0$ origin. The minimum ionization energy for the pyrimidine monomer is near 44 090 cm$^{-1}$ above the $^1B_1(n\pi^*)$ excited state at 31 073 cm$^{-1}$. As can be seen from Fig. 5, features in two of the three regions displayed disappear as the ionization energy is lowered from 44 363 to 42 320 cm$^{-1}$.

Calculations using a LJ–HB potential function yield four planar configurations, a parallel stacked head-to-tail displaced configuration, and a parallel stacked undisplaced configuration with the two pyrimidine molecules rotated 90° with respect to each other. The latter configuration most likely does not contribute to the observed dimer spectrum since it will probably form an excimer. No perpendicular geometry is calculated even with the LJ–HB potential augmented with multipolar terms. Figures 6 and 7 give those calculated geometries for the pyrimidine dimer which can produce the observed spectral features. The parallel displaced geometry shown in Fig. 6 is head-to-tail displaced by

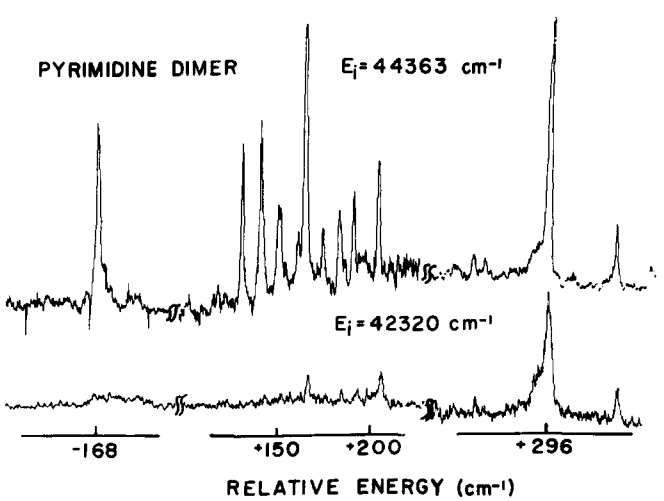


FIG. 5. Three segments of the 2-color TOFMS spectra of the pyrimidine dimer at two ionization energies, top trace at an ionization energy of 44 363 cm$^{-1}$ and the lower trace at an ionization energy of 42 320 cm$^{-1}$. The energy scale is relative to the pyrimidine monomer $0_0^0$.

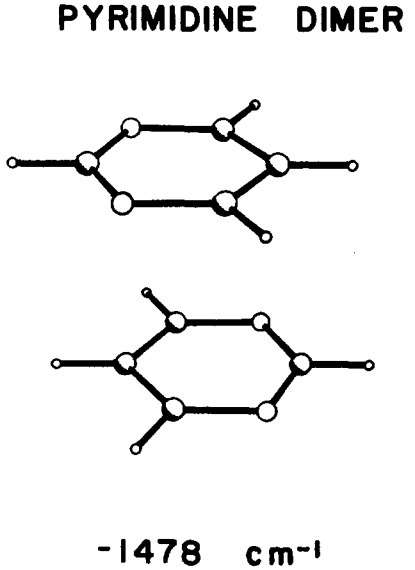


FIG. 6. Minimum energy configuration and binding energy for the stacked pyrimidine dimer as obtained with a LJ plus HB potential calculation.

0.6 Å along the CH–CH line from the molecular center; the interplane separation is 3.3 Å. The calculated binding energy for this dimer is 1478 cm$^{-1}$.

The planar configurations are displayed in Fig. 7. Configuration I has a center to center distance of 5.5 Å, two N---H hydrogen bonds (2.3 Å separation), and a calculated binding energy of 709 cm$^{-1}$. Configurations II, III, and IV also display some hydrogen bonding but to a lesser extent than that displayed in configuration I. In these latter three cases, the less "acidic" hydrogens, not between the two N atoms, are involved in the "hydrogen bonds": the pyrimidine molecule center to center distance is ~6.0 Å and the calculated binding energies range from 400 to 430 cm$^{-1}$, substantially less than the binding energy for configuration I. Configuration II has two N--H hydrogen bonds each of 2.9 Å. Configurations III and IV have a nitrogen atom of one pyrimidine equidistant from two hydrogens of the other pyrimidine with an apparent hydrogen bond distance of 2.9 Å. Planar configurations in which two nitrogens are facing each other are not stable.

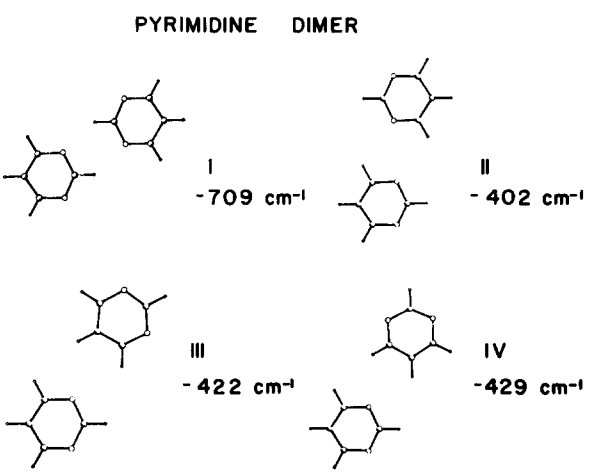


FIG. 7. Minimum energy configurations and binding energies for the planar pyrimidine dimers as obtained with a LJ plus HB potential calculation.

### C. Rotational structure

Rotationally resolved 2-color TOFMS data can be obtained for the pyrazine and pyrimidine monomers using the resolution presently available in our laboratory ($\Delta\nu \sim 0.08$ $cm^{-1}$). The spectra are presented in Fig. 8. These well resolved spectra evidence a central $Q$ branch with well developed $R$ and $P$ branches to the high and low energy sides, respectively. The calculated rotational structures for these transitions are presented in Fig. 9. In order to make the fit look reasonable, a 0.1 $cm^{-1}$ Gaussian linewidth was incorporated in the calculated spectrum.

Considering that a symmetric top equation is used for the fit, the agreement between the calculated and experimental results is excellent. The purpose of this exercise is to observe and calculate the rotational spectrum of a dimer. One can see from Fig. 10 (top) that the rotational structure of the pyrazine dimer is not evident at this laser linewidth. Similar conclusions arise from the spectra of the benzene dimer (see Fig. 11). Computer simulations of the pyrazine dimer spectrum (based on the symmetric top calculations), show that a $\sim 0.005$ $cm^{-1}$ laser linewidth is required to resolve rotational transitions for the aromatic dimers (Fig. 10 bottom). An attempt to fit the rotational contours to parallel or perpendicular transitions of parallel or perpendicular dimers demonstrates that no convincing conclusions concerning dimer geometry can be reached in this manner. In fact, the spectra of the parallel and perpendicular pyrazine dimer origins do not appear different at this resolution. The calculated contours are found using rotational constants of $A'' = 0.0611$, $B'' = 0.0157$, and $C'' = 0.0141$ $cm^{-1}$ for the perpendicular dimer and $A'' = 0.0381$, $B'' = 0.0153$, and $C'' = 0.0112$ $cm^{-1}$ for the parallel planar dimer.

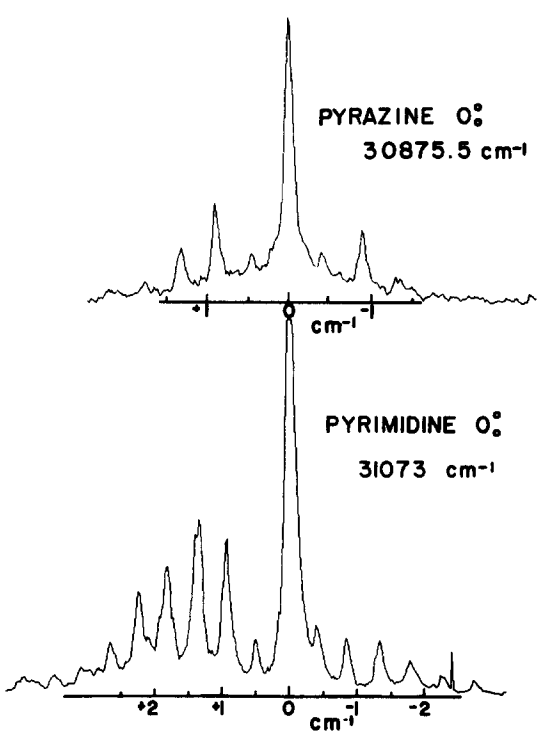


FIG. 8. Two-color TOFMS rotational spectra of the origins of pyrazine (top) and pyrimidine (bottom) monomers.

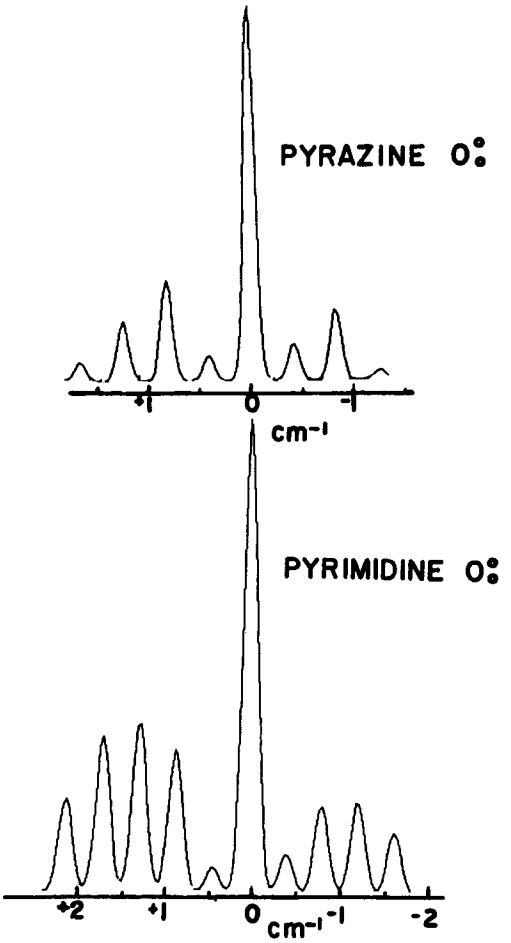


FIG. 9. Simulated rotational spectra of the pyrazine and pyrimidine origins.

## IV. DISCUSSION

### A. Pyrazine dimer

In the following paragraphs, only the pyrazine-$h_4$ dimer results will be discussed in detail. The similarity between the pyrazine-$h_4$ and -$d_4$ dimer results obviates the need for discussion of these data separately.

One of the most important experimental observations concerning the pyrazine dimer is the change in the spectrum as a function of ionization laser or second photon energy. Lowering the ionization laser energy by 1000 $cm^{-1}$ to 42 185 $cm^{-1}$ causes three features to disappear: two of these are assigned as vibrations built on a single origin (see Table I and Fig. 1). Further reduction of the ionization energy to 41 721 $cm^{-1}$ results in no observed TOFMS spectrum for the pyrazine dimer. At least two different geometries of the pyrazine dimer are therefore present in the beam. The dimer with the higher ionization energy is probably a symmetrical dimer with two symmetry equivalent molecules because only one origin is associated with the high ionization energy spectrum.

Different geometries will possess different ionization energies depending on the involvement of the $\pi$ clouds in the overall dimer interaction. For example, a planar hydrogen bonded dimer would probably have a poor ion "solvation" or stabilization and might therefore have a higher ionization energy. This geometry would in addition have only one spec-

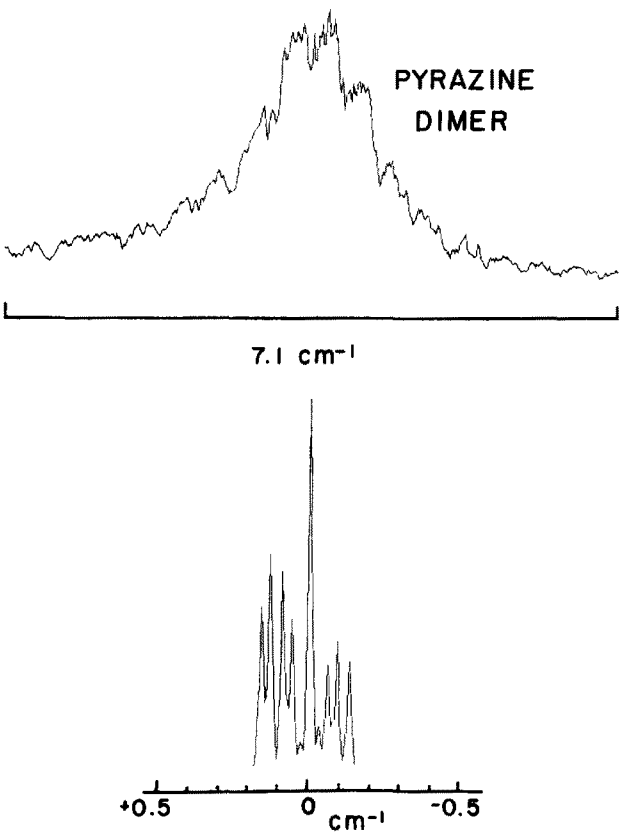


FIG. 10. Two-color TOFMS rotational spectrum of the pyrazine dimer origin (top) and computer simulated rotational spectra of the pyrazine dimer origin (bottom). The origin is at 30 849.5 $cm^{-1}$ ( $-26.5$ $cm^{-1}$ origin in Fig. 1). The FWHM is roughly 2 $cm^{-1}$. The 30 865.0 $cm^{-1}$ origin looks nearly identical to this one at the experimental resolution.

troscopic origin. A perpendicular geometry dimer would, on the other hand, probably evidence two features and a lower ionization energy due to the $\pi$-cloud involvement of the "horizontal" pyrazine in the stabilization of the ion.

The calculations give three general geometries for the pyrazine dimer: a parallel planar, a perpendicular, and a parallel stacked on 90° rotated geometry. The latter geometry is not discussed in this work because it likely is not important for any of the spectroscopic observations presented earlier. The remaining two configurations give rise to three separate spectra: one for the parallel planar geometry (I) and two for the perpendicular geometry (base IIa and stem IIb).

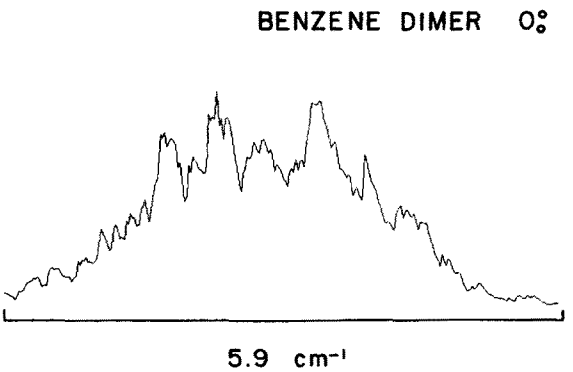


FIG. 11. Two-color TOFMS of the benzene dimer $0_0^0$ transition at 0.08 $cm^{-1}$ resolution. Most of the "features" in this trace are noise and are not reproducible.

TABLE I. Pyrazine dimer.

| Energy (vac. $cm^{-1}$) | Energy relative to corresponding pyrazine feature ($cm^{-1}$) | Energy relative to corresponding pyrazine dimer feature ($cm^{-1}$) | Assignments[a] |
|---|---|---|---|
| 30 849.5 | −26.5 | 0 | II base $0_0^0$ |
| 30 865.0 | −11.0 | 0 | I $0_0^0$ |
| 30 870.2 | −5.8 | 20.7 | |
| 30 879.1 | 3.1 | 29.6 | |
| 30 888.0 | 12.0 | 23.0 | |
| 30 891.4 | 15.4 | 41.9 | |
| 30 898.7 | 22.7 | 49.2 | |
| 30 902.3 | 26.3 | 37.3 | |
| 39 910.1 | 34.1 | 0 | II stem $0_0^0$ |
| 30 914.0 | 38.0 | 3.9 | |
| 30 918.2 | 42.2 | 8.1 | |
| 30 926.7 | 50.7 | 16.6 | |
| 31 228.5 | −30.5 | 0 | II base $10a_0^1$ |
| 31 238.5 | −20.5 | 0 | I $10a_0^1$ |
| 31 245.4 | −13.6 | | |
| 31 254.8 | −4.2 | | |
| 31 289.4 | 30.4 | 0 | II stem $10a_0^1$ |
| 31 297.6 | 38.6 | | |
| 31 314.4 | 55.4 | | |
| 31 433.3 | −26.4 | 0 | II base $6a_0^1$ |
| 31 445.1 | −14.6 | 0 | I $6a_0^1$ |
| 31 456.8 | −2.9 | | |
| 31 467.8 | 8.1 | | |
| 31 481.7 | 22.0 | | |
| 31 488.9 | 29.2 | | |
| 31 493.2 | 33.5 | 0 | II stem $6a_0^1$ |
| 31 507.9 | 48.2 | | |
| 31 565.7 | 106.0 | | |
| 31 677.9 | −21.1 | 0 | II base $10a_0^2$ |
| 31 686.1 | −12.9 | 0 | I $10a_0^2$ |

[a] See Fig. 4.

Table I gives the assignment of the dimer spectra. The planar geometry (I) is assigned to the origin at $-11$ $cm^{-1}$ (Fig. 1) since this single origin feature is associated with the higher ionization energy. The other two origins at $-26.5$ and $+34.1$ $cm^{-1}$ (Fig. 1) with respect to the pyrazine monomer origin are assigned to the perpendicular dimer because they both show the same low ionization energy. The base (IIa) is associated with the red shifted origin and the stem (IIb) is associated with the blue shifted origin. This latter correlation between spectra and calculated structures is based on the argument presented in previous publications[1,2] relating solvent cluster shifts and $\pi$-cloud involvement in the solute–solvent interaction: the larger the red shift, the more direct is the interaction between the system and the solvent. Thus the base molecule should be expected to have a larger red shift than the stem molecule.

The pyrazine $6a^1$ (in-plane C–C stretch) and $10a^1$ (out-of-plane C–C bend) vibrational modes show strong interaction with the van der Waals modes (Fig. 3).

### B. Pyrimidine dimer

The ionization energy for the pyrimidine dimer system is again an important piece of information used to help determine the number of different configurations responsible for

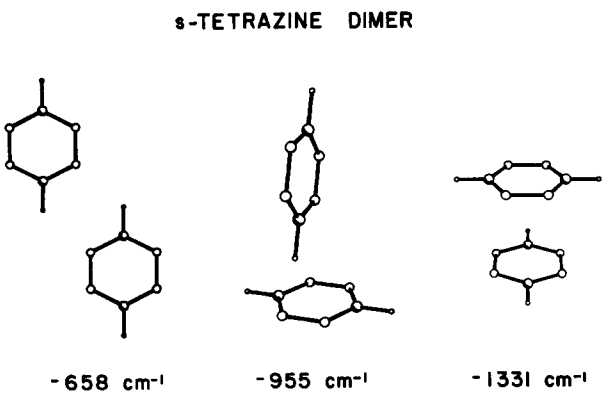


FIG. 12. Minimum energy configurations and binding energies for the tetrazine dimer as obtained with a LJ plus HB potential calculation.

the observed spectra and, perhaps, their geometry. Lowering the ionization by 2 043 $cm^{-1}$ to 42 320 $cm^{-1}$ causes the feature at $-168\ cm^{-1}$ to disappear, the features at $\sim +175\ cm^{-1}$ nearly to disappear, and the feature at $+296\ cm^{-1}$ to reduce in intensity. In addition, dimer spectral shifts can also be employed to associate calculated geometries with spectroscopic features: red shifted origins can be assigned to parallel stacked geometries, and blue shifted origins to planar hydrogen bonded forms. Perpendicular geometries can be responsible for both red and blue shifts depending on which molecule of the dimer is involved.[1]

LJ–HB potential calculations suggest one parallel stacked head-to-tail displaced, one parallel stacked rotated, and four parallel planar configurations for the pyrimidine dimer. No perpendicular geometry can be calculated using LJ–HB or a multipolar form.[1,2] All calculations give nearly identical geometries and binding energies for the parallel planar and stacked configurations.

The features at $-168\ cm^{-1}$ is suggested to be due to the parallel stacked and displaced head-to-tail geometry. One would expect this structure to have only one spectroscopically observed $0_0^0$ transition and a substantial red shift. The remaining features in the spectra, due to their significant blue shifts, must be attributed to planar hydrogen bonded dimers. The feature at $+296\ cm^{-1}$ is suggested to be due to configuration I shown in Fig. 7. This configuration of the pyrimidine dimer forms two hydrogen bonds both of which involve the hydrogen atoms between the two ring nitrogen atoms on each pyrimidine: these hydrogens are the most electropositive (acidic) hydrogens on the ring. This configuration also has the monomers closest to each other (5.5 Å compared to 6.0 Å in the others). These factors suggest that configuration I gives rise to the most blue shifted feature in the spectra. The remaining three configurations II, III, and IV must generate the features in the $+175\ cm^{-1}$ region. Configuration II is a symmetrical dimer and will account for one feature while configurations III and IV each will account for two features since the pyrimidines in these last two configurations are not symmetry equivalent. Assigning these features to configurations II, III, and IV is a difficult task without further information: five of the eight major features in this region can, however, be associated with origins of configurations II, III, and IV.

The parallel planar hydrogen bonded configuration I is assigned to the large blue shift, low ionization energy feature, and the parallel stacked displaced geometry is assigned to the large red shifted, high ionization energy feature. On the other hand, the parallel planar pyrazine dimer is assigned to the feature with the higher ionization energy (and also a small red shift). Clearly the two dimers have a very different electronic structure and the component monomers must interact in a different manner. A possible explanation for these apparent differences is that the N–C–N moiety of the pyrimidine system becomes the positive end of the molecular ion which is in turn well solvated in the parallel planar dimer thus lowering the ionization energy, and that the loss of electron density in the N–C–N region in the $n\pi^*$ excited state reduces the hydrogen bond energy thus increasing the energy of the excited $S_1$ state and causing a dimer blue shift. Similar arguments can be rendered to rationalize a negligible shift for the pyrazine system. We caution, however, that all such qualitative reasoning is subject to verification by more rigorous quantum mechanical calculations.

To ensure that our LJ–HB potential can produce other perpendicular dimer configurations, we have calculated the geometries expected for the tetrazine system. The tetrazine dimer has been studied by Levy and co-workers,[3] who have reported two geometries: a parallel planar configuration and a perpendicular configuration. These experiments involve rotationally resolved fluorescence excitation spectra. Our calculations generate three geometries for this dimer: a parallel planar configuration, a parallel, stacked and 90° rotated configuration, and a perpendicular configuration, as shown in Fig. 12. The calculated perpendicular configuration has one hydrogen of the stem tetrazine pointing towards an N–N

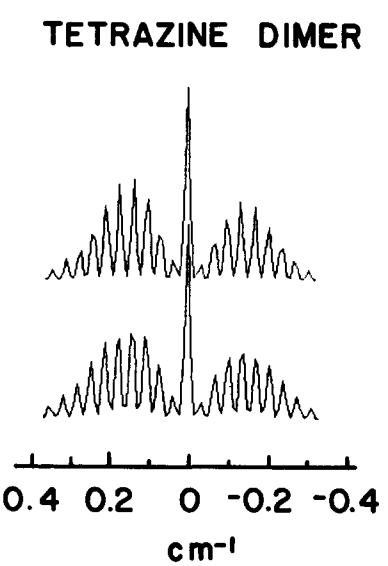


FIG. 13. Calculated rotational contours of the parallel polarized transition of the perpendicular tetrazine dimer centered at 18 272.0 $cm^{-1}$ (0 $cm^{-1}$ in the figure). The upper trace is calculated using the rotational constants obtained from the perpendicular configuration reported in Ref. 3(a). The lower trace is calculated using the rotational constants obtained from the perpendicular configuration reported in this work. A symmetric top model is assumed for both calculations and the intensities used are those of Ref. 3(a). The rotational constants employed are given in the text; in the symmetric top approximation $\bar{B}'' = (B'' + C'')/2$.

bond of the base tetrazine. In this configuration the plane of the stem tetrazine bisects the two N–N bonds of the base tetrazine. Levy's published perpendicular configuration[3(a)] has one hydrogen of the two C–H bonds of the stem tetrazine pointing toward one C–H bond of the base tetrazine and the plane of the stem tetrazine passing through the two C–H bonds of the base tetrazine. Rotational constants reported by Levy and obtained from a rotational analysis of the perpendicular configuration for parallel polarization are $A'' = 0.072\,87$ $cm^{-1}$, $B'' = 0.017\,22$ $cm^{-1}$, and $C'' = 0.016\,49$ $cm^{-1}$. Rotational constants obtained from our calculated perpendicular configuration are $A'' = 0.064\,58$ $cm^{-1}$, $B'' = 0.016\,44$ $cm^{-1}$, and $C'' = 0.018\,466$. These two sets of rotational constants render reasonably similar spectra, as can be seen in Fig. 13.

## V. CONCLUSION

The analysis of the structure and properties of the pyrazine and pyrimidine dimers is based on an interpretation of ionization energy dependence, van der Waals vibronic structure, dimer spectral shifts, and potential energy calculations with LJ–HB and multipolar forms.

Variation of the ionizing laser energy allows different configuration dimers of a particular species to be identified. The pyrazine ($h_4$ and $d_4$) dimer has two identified geometries based on ionization energy dependence and vibronic analysis. Given the dimer spectral shifts and calculations, these have been associated with a planar parallel hydrogen bonded configuration and a perpendicular configuration. A third geometry, planar stacked and rotated 90°, is calculated but not observed probably due to excimer formation.

The pyrimidine dimers absorb in three spectral regions. The lowest energy feature is thought to be the calculated head-to-tail parallel stacked displaced geometry, the highest energy feature is assigned as a parallel planar strongly hydrogen bonded form in which the most electropositive H atoms are involved in the hydrogen bonding. The features at $+175$ $cm^{-1}$ are attributed to different planar configurations which are only weakly hydrogen bonded through the less acidic hydrogens on the rings.

Dimer spectral shifts are expected to follow the rules determined previously for solute–solvent clusters: the major red shift mechanism is $\pi$-system coordination or overlap between the two molecules and the major blue shift mechanism is hydrogen bonding. Ionization energies can be rationalized in accordance with the general notions of ion solvation by either the $\pi$ system in the case of pyrazine or the N–C–N hydrogen bonding region in the case of pyrimidine.

Calculations are also presented for the tetrazine dimers to compare parallel planar and perpendicular spectroscopically assigned geometries and our calculations. Calculations predict, and experiments suggest, perpendicular geometries for toluene, benzene–toluene, pyrazine, and tetrazine but not for benzene. Moreover, calculations predict, and experiments are consistent with, the absence of perpendicular geometries for the pyrimidine dimer. Perhaps one of the most remarkable results of this study is the rather large number of different, roughly equal binding energy configurations found for the N-heterocyclic aromatic dimers in general.

[1]K. S. Law, M. Schauer, and E. R. Bernstein, J. Chem. Phys. **81**, 4871 (1984).
[2]M. Schauer and E. R. Bernstein, J. Chem. Phys. **82**, 3722 (1985).
[3](a). C. A. Haynam, D. V. Brumbaugh, and D. H. Levy, J. Chem. Phys. **79**, 1581 (1983); (b). L. Young, C. A. Haynam, and D. H. Levy, *ibid.* **79**, 1592 (1983).
[4]Y. D. Park and D. H. Levy, J. Chem. Phys. **81**, 5527 (1984).
[5]D. V. Brumbaugh, C. A. Haynam, and D. H. Levy, J. Chem. Phys. **73**, 5380 (1980).
[6]D. E. Poelti and J. K. McVey, J. Chem. Phys. **78**, 4349 (1983).
[7]Y. Tomioka, H. Abe, N. Mikami, and M. Ito, J. Phys. Chem. **88**, 5186 (1984).
[8]J. Wanna and E. R. Bernstein, J. Chem. Phys. **84**, 927 (1986).
[9](a). F. A. Momany, L. M. Carruthers, R. F. McGuire, and H. A. Scheraga, J. Phys. Chem. **78**, 1595 (1974); (b) G. Nemethy, M. S. Pottle, and H. A. Scheraga, *ibid.* **87**, 1883 (1983).
[10]F. Mulder, G. Van Dijk, and C. Huiszoon, Mol. Phys. **38**, 577 (1979).
[11]G. Herzberg, *Molecular Spectra and Molecular Structure. II. Infrared and Raman Spectra of Polyatomic Molecules* (Van Nostrand Reinhold, New York, 1945), Chaps. I and IV.
[12]P. J. Wheatley, Acta Crystallogr. **10**, 182 (1957).
[13]P. J. Wheatley, Acta Crystallogr. **13**, 80 (1960).